THE JOURNAL OF BIOLOGICAL CHEMISTRY
Vol. 278, No. 39, Issue of September 26, pp. 38022–38028, 2003

Printed in U.S.A.

Plasmodium falciparum Falcilysin

A METALLOPROTEASE WITH DUAL SPECIFICITY*

Received for publication, June 26, 2003, and in revised form, July 17, 2003
Published, JBC Papers in Press, July 22, 2003, DOI 10.1074/jbc.M306842200

Christina E. Murata and Daniel E. Goldberg‡

From the Howard Hughes Medical Institute, Washington University, Departments of Molecular Microbiology and Internal Medicine, St. Louis, Missouri 63110

The malaria parasite *Plasmodium falciparum* degrades host cell hemoglobin within an acidic food vacuole. The metalloprotease falcilysin has previously been identified as an important component of this catabolic process. Using random peptide substrate analysis, we confirm that recombinant falcilysin is highly active at acidic pH, consistent with its role in hemoglobin degradation. Unexpectedly, the enzyme is also robustly active at neutral pH, but with a substantially different substrate specificity. Imaging studies confirm the location of falcilysin in the food vacuole and reveal association with vesicular structures elsewhere within the parasite. These data suggest that falcilysin may have an expanded role beyond globin catabolism and may function as two different proteases in its two locations.

Plasmodium falciparum is the causative agent of the deadliest form of human malaria. Each year 500 million infections and up to 2 million deaths are attributed to *Plasmodium* parasites (1). This disease is a major public health issue in many areas of the world where the increasing prevalence of drug-resistant strains underscores the need to identify new drug targets. Examination of the parasite's unique metabolic pathways, such as hemoglobin degradation, provides numerous attractive candidates for chemotherapeutic development.

Plasmodium infects and develops within human erythrocytes where hemoglobin is degraded in a semi-ordered cascade of proteases to provide energy and nutrients to the growing parasite (2). Hemoglobin degradation occurs in the unique acidic environment of the food vacuole. A family of aspartic proteases, the plasmepsins, mediates the initial cleavage within a conserved hinge region of the hemoglobin alpha chains (3, 4). The denatured globin is further degraded by plasmepsins in concert with a family of cysteine proteases, falcipain-2 and -3 (2, 4–7). The resulting globin peptides serve as substrates for the zinc metalloprotease falcilysin (FLN).[1] FLN prefers to degrade small globin peptides up to 20 amino acids in length at a pH optimum of 5.2 (8), consistent with the acidic environment of the food vacuole (9, 10). The temporal expression pattern of FLN is similar to that of other globinases yet differs by the absence of proteolytic processing during biosynthesis (11).

FLN is a member of the M16 family of the clan ME zinc metalloproteases. This family is characterized by an inverted active site motif of H*XX*EH (12), where the two histidines and a glutamic acid residue located 75–84 residues C-terminal to this motif are involved in coordinating the catalytic zinc ion. The M16 family is divided into subfamilies A and B. Subfamily B includes the mitochondrial processing peptidase (MPP) and the chloroplast stromal processing peptidase; both enzymes are involved in removing N-terminal targeting peptides (13–15). Falcilysin belongs to subfamily A whose members are oligoendopeptidases involved in processing biologically important peptides such as yeast α factor (16, 17), insulin (18), and transforming growth factor α (19). All of the subfamily A members are large enzymes (greater than 100 kDa) with the catalytic machinery located in the N terminus. The function of the C terminus remains unknown.

In the current study we explore the substrate preferences of FLN. These studies reveal a bimodal pH optimum with starkly different substrate specificities for acidic and neutral pH conditions. Immunolocalization studies reveal a second location for FLN, outside of the acidic food vacuole. These data point to the possibility of an expanded role for this protease in *Plasmodium falciparum* biology.

MATERIALS AND METHODS

Culture of Parasites

P. falciparum clone HB3 (Honduras, gift of W. Trager, Rockefeller University) was cultured using the methods of Trager and Jensen (20) in serum-free Roswell Park Memorial Institute media supplemented with 0.5% Albumax (Invitrogen, Grand Island, NY). Synchrony was maintained with sorbitol treatment (21).

Antibody Production and Specificity

The affinity-purified A1219T antibody was generated as previously described (11). For generation of 1624T, polyclonal rabbit antiserum was raised (CoCalico Biologicals, Reamstown, PA) against a synthetic eight-branch multiple antigenic peptide (MAP) peptide containing residues 603–612 of FLN (KKRIENFNEQ) (Invitrogen, Carlsbad, CA).

Immunofluorescence Microscopy

Infected RBCs at the trophozoite stage were prepared as previously described (22). Samples were immunolabeled with rabbit anti-FLN (A1219T, 1:10, or 1624T, 1:1000), mouse anti-PM IV (13.9.2 1:10), rat anti-Bip (1:1000, MR4, J. H. Adams). Secondary antibodies used for detection included fluorescein isothiocyanate-conjugated goat anti-mouse IgG, Alexa 594 goat anti-rabbit IgG (Molecular Probes, Eugene, OR), Alexa 488 anti-rat IgG, and Alexa 488 goat anti-mouse IgG. Coverslips were mounted in Vectashield with DAPI (Vector Laboratories, Burlingame, CA) and viewed using a Zeiss axioscope microscope at 1000× magnification. Both αFLN antibodies gave similar results. There was no difference in FLN distribution in trophozoites or schizonts.

* This work was supported in part by the National Institutes of Health Grant AI-47798 (to D. E. G.). The costs of publication of this article were defrayed in part by the payment of page charges. This article must therefore be hereby marked "*advertisement*" in accordance with 18 U.S.C. Section 1734 solely to indicate this fact.

‡ A recipient of a Burroughs Wellcome Fund Scholar Award in Molecular Parasitology. To whom correspondence should be addressed: Howard Hughes Medical Institute, Washington University Medical School, Departments of Molecular Microbiology and Medicine, Campus Box 8230, 660 S. Euclid Ave., St. Louis, MO 63110. Tel.: 314-362-1514; Fax: 314-367-3214; E-mail: goldberg@borcim.wustl.edu.

[1] The abbreviations used are: FLN, falcilysin; MPP, mitochondrial processing peptidase; RBC, red blood cell; DAPI, 4′,6-diamidino-2-phenylindole; PBS, phosphate-buffered saline; ER, endoplasmic reticulum; EM, electron microscopy; MMP, metalloprotease.

Immunoelectron Microscopy

Infected RBCs were processed as described previously (22) except for the fixation, which used 4% paraformaldehyde/0.1% glutaraldehyde, and the staining, which utilized 0.3% uranyl acetate/2% methyl cellulose. Immunolabeling used rabbit anti-FLN (1624T, 1:1000) and rat anti-Bip (1:1000) with species-specific 18- and 12-nm colloidal gold-conjugated secondary antibodies, respectively.

Membrane Extraction

Synchronized mid-stage trophozoite culture ($\sim 5 \times 10^8$ parasites) was labeled with 150 μCi/ml [^{35}S]methionine/cysteine (PerkinElmer Life Sciences, Boston, MA). After a 4-h incubation at 37 °C, parasites were harvested in a 10 mM phosphate buffer (pH 7.1) with protease inhibitors. Parasites were disrupted via sonication and divided into equal portions, which were centrifuged for 1 h at 214,000 $\times$ *g* at 4 °C. The resulting pellets were resuspended in 0.5 ml in one of several solutions: PBS, 0.5 M NaCl in PBS, 100 mM Na_2CO_3 (pH 11), or 1% Triton X-100 in PBS. Extraction proceeded for 1 h on ice followed by a second 214,000 $\times$ *g* centrifugation for 1 h at 4 °C. The resulting supernatant and pellet fractions were retained. The pellets were solubilized with 1% SDS. Immunoprecipitations with antiserum A1219T (23) and autoradiography followed.

Peptide Library Synthesis

An N-terminal acetylated and C-terminal biotinylated random 10-mer peptide with an isokinetic mixture of 19 amino acids (except cysteine) was synthesized by Dr. Chistoph Turk (University of California, San Francisco). This library was used to determine the P′ motifs. Second generation libraries with fixed P′ positions and five random residues in the P positions were generated at the Tufts University protein core facility (Boston, MA). These libraries had free N termini and biotinylated C termini. The second generation libraries were used to predict preferred residues in the unprimed positions. The predicted optimal substrates were synthesized with DABCYL and EDANS modifications (24) by AnaSpec Inc. (San Jose, CA) for use in kinetic studies.

Peptide Library Cleavage Assays

To Determine the P′ motifs—50 pmol of purified recombinant FLN (11) was incubated with 100 nmol of N-terminally acetylated random 10-mer substrate in 100 mM NaOAc, pH 5.2 (acidic conditions), or 100 mM bis-Tris, pH 7.2 (neutral conditions), in 400 μl. Cleavage reactions were incubated at 37 °C for 4 h; samples were then heated to 100 °C for 3 min. Cleavage products were analyzed by Edman degradation (Midwest Analytical, St. Louis, MO). Control pH titrations with the buffers used in these experiments showed insignificant buffer effects on enzyme activity.

Amino acid preference for a single position was determined by subtracting a residue's raw abundance in the cleavage reaction from the abundance of the same residue in a control, enzyme-free reaction, which eliminates bias for amino acids eluting at positions with background interference. This corrected abundance was divided by the prevalence of that residue within the 10-mer library, to control for bias present within the library. These data were then normalized to an average amino acid abundance of 1. Similar results were obtained using incubations of 0.5 h and overnight. The data shown are the average of three incubations.

To Determine the P motif—Each experiment with a second generation library used substrate incubated with purified rFLN (1000:1 molar ratio), as well as no-enzyme reactions. Incubations proceeded in 100 mM NaOAc, pH 5.2 (acidic conditions), or 100 mM bis-Tris, pH 7.2 (neutral conditions), at 37 °C overnight; samples were then heated to 100 °C for 3 min. The sample with enzyme and substrate, along with a substrate-only sample, were incubated with an excess of avidin-Sepharose (0.6 ml) (Pierce, Rockford, IL) for 1 h at room temperature to remove the C-terminal portion of the cleavage product along with any uncleaved substrate prior to N-terminal sequence analysis.

The abundance of each amino acid was quantified for each position in the cleavage product by first subtracting the abundance of each residue from the library background (substrate only plus avidin). Next, the percent abundance of each corrected residue was divided by the abundance of the same corrected residue in the control, enzyme-free reaction without avidin pull-down. These data were also normalized to 1. There were three independent determinations of the unprimed motif. The data shown represents the average of these experiments.

Single Substrate Kinetic Assays—3.5 nM purified rFLN was incubated with the quenched fluorogenic peptides (final concentrations ranging from 0.031 μM to 30 μM) in the presence of 100 mM NaOAc, pH 5.2, or 100 mM bis-Tris, pH 7.2, at 37 °C. Each concentration was tested in duplicate or triplicate. A PerkinElmer Life Sciences LS50B fluorimeter with an excitation wavelength of 336 nm (slit width 5) and emission detection at 490 nm (slit width 8) was used to monitor the generation of cleavage products in real-time at 37 °C. The cleavage reaction was followed for 50 s. K_m and V_{max} were determined by measuring the initial velocities of product appearance. Apparent k_{cat} values were calculated ($k_{cat} = V_{max}/[E]$) using the purified enzyme protein concentration (BCA, Pierce) as an estimate of active enzyme. Kinetic analyses were also performed with the optimized substrates over a range of pH conditions with overlapping buffers: pH 3.6–5, NaOAc; pH 5–7, bis-Tris; pH 7–10, Tris. Optimized substrates were compared with fluorogenic α74–75 (AHVD ↓ DFPN) (8), a known FLN globin peptide substrate. rFLN exhibited poor activity (k_{cat}/K_m several fold lower than for α74–75) against a decameric version of this globin peptide.

RESULTS

Determination of FLN optimal P′ Motifs—Random peptide libraries provide a facile tool to probe enzyme function and selectivity. Previous data indicated that FLN displayed good activity with globin peptide substrates at pH 5.2 but fared poorly with the same substrates at neutral pH (8). Moreover, falcilysin globin substrates lack a strong consensus sequence (8). We therefore pursued a strategy similar to that of Turk *et al.* (25) to refine FLN cleavage specificity at acidic pH and to investigate the possibility of activity and specificity at neutral pH. Experiments were carried out at pH 5.2 to mimic the pH of the food vacuole and at pH 7.2 to reflect conditions in the rest of the parasite. A random 10-mer library was utilized to determine the primed (P′) side motif of substrates, and a second generation library with fixed P′ positions was used to identify the unprimed (P) motif.

As described under "Materials and Methods," an N-terminal-acetylated, C-terminal-biotinylated random 10-mer library was used to identify residues preferred in the P′ positions. As shown in Fig. 1*A*, FLN strongly favors bulky hydrophobic amino acids in the P1′ position at both acidic and neutral pH. At P2′, FLN prefers hydrophobic residues at pH 5.2; at pH 7.2, these same residues are abundant but Arg is more strongly preferred. Hydrophobic residues, especially Met, predominate in the P3′ position at both pH conditions. At P4′ and P5′, there is a strong selection of acidic residues at pH 5.2. At neutral pH, the enzyme is much less selective at these positions. An optimal motif for FLN under acidic conditions is FFMEE and under neutral pH conditions is FRMRG.

Second Generation Libraries Reveal the FLN P Motif—To determine a motif for the unprimed positions, a second generation C-terminal-biotinylated library was constructed using the P′ motifs and randomized amino acids in the P positions. As shown in Fig. 1*B*, FLN strongly favors Ser in the P1 position under both acidic and neutral conditions. At the P2 position, Met and His were the most abundant amino acids generated at acidic pH, whereas Asn and His were preferred at neutral pH. At the P3 position, acidic conditions yielded Glu and His; neutral conditions favored Arg and Gly. Asn was highly preferred at the P4 position at pH 5.2. In contrast, neutral pH conditions favored several residues, most prominently Lys. Tyr was the most abundant residue in the P5 position under acidic conditions while Met was highly preferred with neutral conditions. These experiments predict an optimal motif for acidic pH of YNEHS ↓ FFMEE. A substrate with the sequence MKRHS ↓ FRMRG should provide optimal cleavage at neutral pH.

Kinetic Analysis of Optimized Substrates—Peptide library predictions can be evaluated by measuring the kinetic capabilities of optimized substrates. Our standard of comparison is the peptide α74–75, which is a sequence in the hemoglobin alpha chain recognized by FLN for cleavage (8). To assess the contribution and overall importance of both the P and P′ portions of the optimized substrates, we synthesized substrates with a

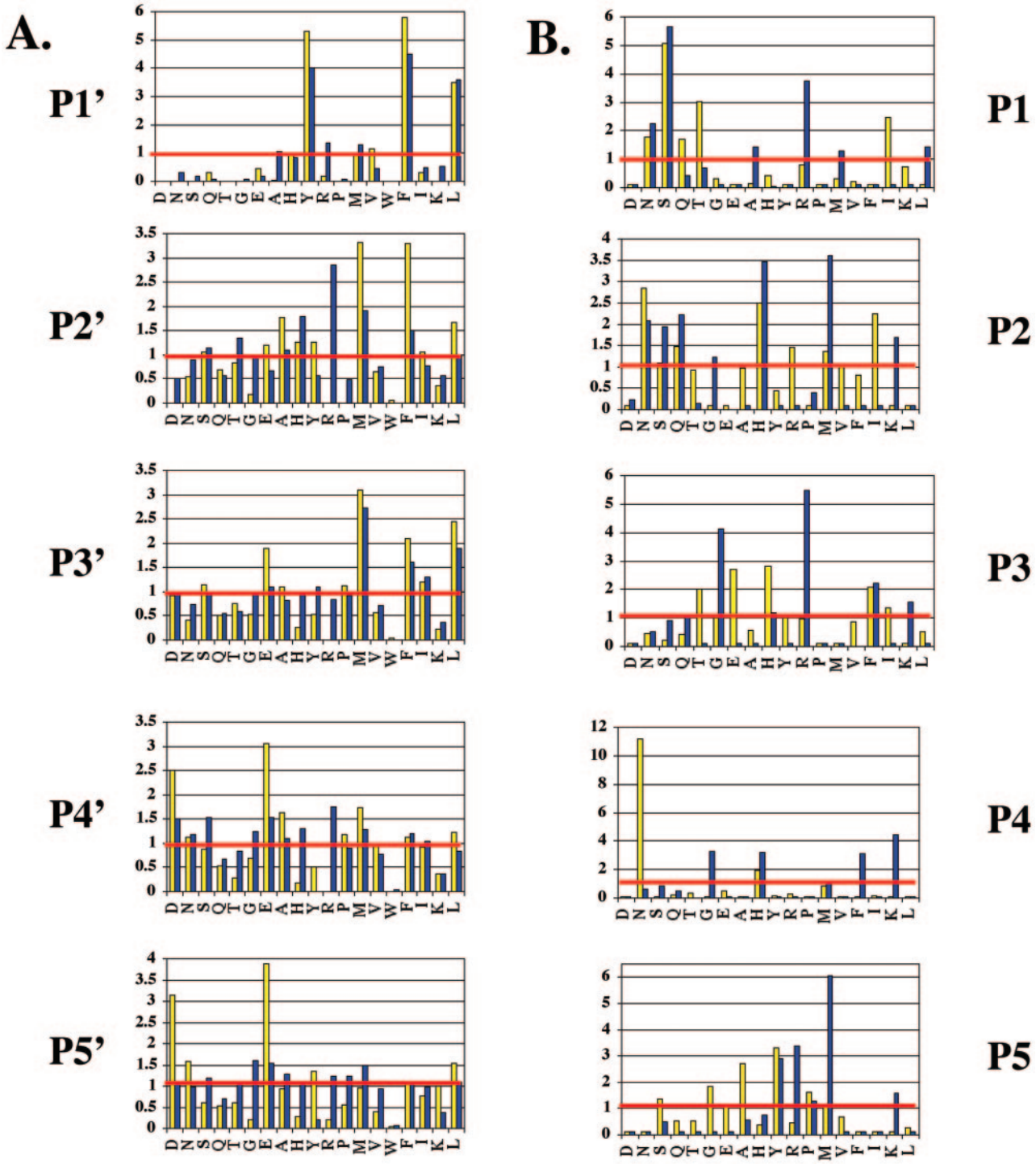

FIG. 1. **FLN P′ and P motifs differ under acidic and neutral pH.** Data for each primed (*P1′* to *P5′*) and unprimed (*P1* to *P5*) position, where recombinant enzyme was incubated with the random 10-mer peptide library under acidic (pH 5.2) or neutral (pH 7.2) conditions. Cleavage products were analyzed and quantified by Edman degradation. Data were normalized to 1, which represents the average amount of amino acid released in a given position. Amino acid abundance is depicted on the *y*-axis, and the one-letter amino acid symbols are on the *x*-axis. Acidic pH data are shown in *yellow*; neutral pH data are shown in *blue*. The *red line* demarcates an abundance of 1; residues at this level are neither preferred nor disfavored.

combinatorial approach. Our hypothesis, based on the published experience with other metalloproteases, was that the P motif would be the most important in determining overall catalytic efficiency. Furthermore, we predicted that a sequence optimized under one pH condition would not be as efficient at the opposite pH. The use of quenched fluorogenic substrates enabled us to kinetically assess each substrate by measuring the cleavage in real-time (Table I).

Analysis of α74–75-based substrates optimized in the P′ positions revealed that manipulation of these C-terminal sequences alone can confer a significant increase in the overall catalytic efficiency. Optimization with the P′ acid sequence (74–75/P′acid) led to a 5.5-fold increase in k_{cat}/K_m at pH 5.2. The P′ neutral sequence (74–75/P′neut) bestowed a striking 24-fold increase in catalytic efficiency at pH 7.2. These increases arose mostly from a lower K_m, because k_{cat} values remained within the same range. When each substrate was tested at the opposite pH from which it was optimized, there

TABLE I
Kinetic summary of optimized peptides

K_m and k_{cat} values were determined by fitting initial rate data from multiple substrate concentrations to the Michaelis-Menten equation. k_{cat} values are apparent because the active enzyme was estimated from the protein concentration of the purified preparation.

	pH	K_m μM	k_{cat} s^{-1}	k_{cat}/K_m M^{-1} s^{-1}
α74-75	5.2	11.5 ± 1.37	9.5×10^{-3}	824
AHVD ↓ DFPN	7.2	15.3 ± 5	3.3×10^{-3}	216
74-75/P′acid	5.2	0.51 ± 0.05	2.31×10^{-3}	4,529
AHVD ↓ FFMEE	7.2	1.7 ± 0.26	1.66×10^{-3}	970
74-75/P′neut	5.2	4.1 ± 0.8	1.87×10^{-3}	457
AHVD ↓ FRMRG	7.2	0.81 ± 0.11	4.23×10^{-3}	5,222
Pacid/74-75	5.2	0.787 ± 0.1	1.67×10^{-2}	21,224
YNEHS ↓ DFPN	7.2	2.09 ± 0.32	3.98×10^{-3}	1,906
Pneut/74-75	5.2	7.42 ± 2	8.9×10^{-3}	1,200
MKRHS ↓ DFPN	7.2	1.07 ± 0.1	6.62×10^{-2}	61,994
Pacid/P′acid	5.2	0.317 ± 0.05	4.69×10^{-2}	147,950
YNEHS ↓ FFMEE	7.2	0.169 ± 0.02	1.36×10^{-2}	80,277
Pacid/P′neut	5.2	6.27 ± 1	2.7×10^{-1}	43,242
YNEHS ↓ FRMRG	7.2	0.972 ± 0.1	3.01×10^{-1}	309,414
Pneut/P′neut	5.2	12.1 ± 2	4.1×10^{-2}	3,371
MKRHS ↓ FRMRG	7.2	0.405 ± 0.04	2.16×10^{-1}	534,532
Pneut/P′acid	5.2	0.5811 ± 0.08	4.1×10^{-2}	70,258
MKRHS ↓ FFMEE	7.2	0.8 ± 0.08	1.61×10^{-2}	202,130

was a decrease in k_{cat}/K_m as compared with the preferred pH (a 4.6-fold decrease for P′acid and an 11-fold decrease with P′neutral). Again, this was mostly attributed to differences in substrate binding. The 74–75/P′acid substrate at the disfavored pH 7.2 was still, however, much more efficient than α74–75 (k_{cat}/K_m of 970 *versus* 194). But α74–75 remained a better substrate than 74–75/P′neut at pH 5.2 (k_{cat}/K_m of 928 as compared with 457). These data suggest that the P′ region of FLN substrates contributes substantively to catalytic efficiency.

Optimization in the P positions of 74–75-based substrates, however, argues that these residues are the greatest determinants of catalytic efficiency (Table I). Pacid/74–75 showed a 23-fold increase in k_{cat}/K_m at pH 5.2, as compared with α74–75. We observed a similar pattern with Pneut/74–75, which produced a 320-fold increase in k_{cat}/K_m at pH 7.2, as compared with α74–75. When each substrate was tested at the "disfavored" pH, we again observed decreases in catalytic efficiency. At pH 7.2, Pacid/74–75 produced an 11-fold decrease in k_{cat}/K_m but remained a better substrate than α74–75 at the same pH. The k_{cat}/K_m for Pneut/74–75 dropped 52-fold when the substrate was placed at pH 5.2. Interestingly, when compared with α74–75 at pH 5.2, Pneut/74–75 had a comparable efficiency (k_{cat}/K_m of 928 and 1200, respectively). The changes in k_{cat}/K_m for these substrates derive both from tighter binding and faster catalysis.

Complete optimization in both the P and P′ positions for acidic pH yielded an 180-fold increase in catalytic efficiency compared with α74–75. This was the result of a lower K_m and a higher k_{cat}. As expected, this substrate performed less efficiently at neutral pH (k_{cat}/K_m of 80,277 *versus* 147,949). This neutral value was still a 414-fold increase in k_{cat}/K_m compared with α74–75 at pH 7.2. The Pneut/P′neut peptide yielded a 2,755-fold increase in k_{cat}/K_m compared with α74–75 at neutral pH. This improvement was a result of tight substrate binding and faster catalysis. At pH 5.2, Pneut/P′neut yielded a 3.6-fold increase in catalytic efficiency compared with α74–75, a 158-fold decrease from the optimal performance of the substrate at pH 7.2. Fig. 2 shows the catalytic efficiencies of Pacid/P′acid and Pneut/P′neut from pH 3.6 to 10. Pacid/P′acid had two peaks of catalytic efficiency, one at pH 5 and the other at pH 7. Pneut/P′neut was dramatically different, exhibiting one broad peak of catalytic efficiency from pH 7 to 8.5.

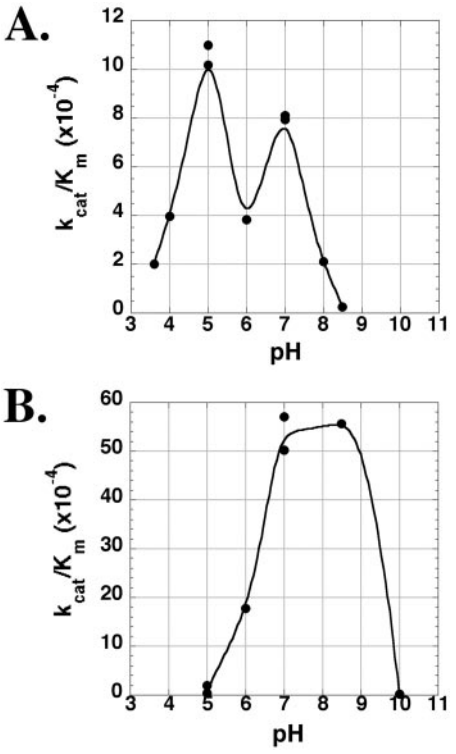

FIG. 2. **Optimized substrates behave differently over a range of pH conditions.** *A*, catalytic efficiency of Pacid/P′acid was measured under a variety of pH conditions. For pH 3.6–5 NaOAc was used, for pH 5–7 bis-Tris was used, and for pH 7–10 Tris was used. Initial velocities were measured in triplicate at multiple substrate concentrations to determine catalytic efficiency. *B*, a similar curve for Pneut/P′neut.

When the Pacid or P′acid motif was joined to the P′neut or Pneut motif, respectively, catalytic efficiency was lower than the fully optimized substrates, as expected (Table I). Optimized substrates with an amino acid substitution were also tested, because sometimes there was more than one preferred residue for a given position (Table II). For the pH 5.2-optimized sequence, we synthesized substrates with a change at the P2 (H to N) and P3 (E to H) positions. For the pH 7.2-optimized

TABLE II
Kinetic summary of substituted peptides
K_m and k_{cat} values were determined by fitting initial rate data from multiple substrate concentrations to the Michaelis-Menten equation.

	pH	K_m μM	k_{cat} s^{-1}	k_{cat}/K_m M^{-1} s^{-1}
P acid/P′acid	5.2	0.317 ± 0.05	4.69×10^{-2}	147,950
YNEHS ↓ FFMEE	7.2	0.169 ± 0.02	1.36×10^{-2}	80,277
P acid HΔN/P′acid	5.2	0.253 ± 0.02	3.26×10^{-2}	128,587
YNENS ↓ FFMEE	7.2	0.239 ± 0.03	1.6×10^{-2}	66,911
P acid EΔH/P′acid	5.2	0.255 ± 0.04	1.87×10^{-2}	73,194
YNHHS ↓ FFMEE	7.2	0.09 ± 0.01	1.52×10^{-2}	169,593
P neut/P′neut	5.2	12.1 ± 2	4.1×10^{-2}	3,371
MKRHS ↓ FRMRG	7.2	0.405 ± 0.04	2.16×10^{-1}	534,532
PneutHΔM/P′neut	5.2	14.81 ± 1.7	2.99×10^{-2}	2,025
MKRMS ↓ FRMRG	7.2	1.28 ± 0.17	3.86×10^{-1}	301,752

sequence, we synthesized a substrate with a change at the P2 position (H to M). Each of these changes gave less than a 2-fold difference in k_{cat}/K_m. These substrates provided strong validation for the optimized sequence predictions generated from the peptide libraries.

Immunofluorescence Suggests Multiple Locations for FLN—FLN was originally purified from food vacuoles. Yet, *in vitro*, falcilysin displayed robust activity at neutral pH. This raised the question of whether FLN might be located in structures outside the acidic food vacuole. Two independent anti-peptide polyclonal antibodies were used to probe the subcellular distribution of falcilysin.

An indirect immunofluorescence signal from the anti-FLN antibody could be detected in the food vacuoles of acetone-fixed cells (Fig. 3*A*), overlapping with the distribution of the food vacuole marker, plasmepsin IV. In addition, an FLN signal was found in vesicular structures within the parasite. Similar vesicular staining was seen with formaldehyde fixation, which would not permeabilize the food vacuole (Fig. 3*B*). The vesicular signal appeared to be specific, because Fig. 3*B* reveals that as little as 10 μg/ml of immunizing peptide was sufficient to block FLN staining. Staining with a second αFLN antiserum, 1624T, gave a pattern similar to that of A1219T. Pre-immune 1624 serum did not detect a signal by immunofluorescence (data not shown). Both antisera were monospecific by immunoblotting (data not shown). These data suggest that falcilysin resides in two locations within the parasite.

Co-localization studies were carried out with BiP, a marker of the endoplasmic reticulum (ER). The distribution of FLN was largely distinct from that of BiP (Fig. 3*C*) and remained so even after treatment with Brefeldin A (data not shown). Furthermore, FLN was confined to the parasite body, because signal from LWL-1, a marker of the parasitophorous vacuolar membrane, surrounded the FLN staining (Fig. 3*D*). Cryo-immunoelectron microscopy (EM) corroborated the immunofluorescence data; by EM, FLN localized to the food vacuole (Fig. 4*A*) and other vesicular structures within the parasite (Fig. 4, *B* and *C*). Again, FLN and BiP had minimal overlap.

FLN Is a Peripheral Membrane Protein—Membrane extraction experiments were performed using radiolabeled trophozoite sonicates (Fig. 5). With PBS and 0.5 M NaCl extractions, FLN remained associated with the pellet. However, extraction in pH 11 carbonate resulted in a shift of FLN into the soluble, or supernatant fraction. FLN was detected in the supernatant fraction after 1% Triton X-100 detergent lysis (data not shown). This stands in contrast to mature plasmepsin I, which in these studies (not shown) and previous work (23) was detected in the supernatant fractions with all extraction conditions. These data indicate that FLN is peripherally associated with membranes.

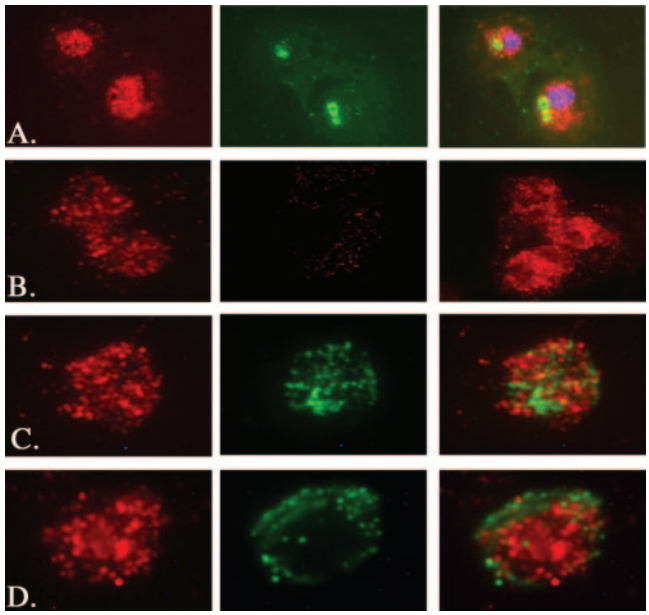

FIG. 3. **FLN localizes to the food vacuole and other vesicular structures.** *A*, indirect immunofluorescence using parasites fixed in acetone. FLN (A1219T) staining is *red* (*left panel*); PMIV staining is *green* (*center*). The *merged image* (*right panel*) has additional nuclear staining (DAPI) in *blue*. *B*: *Left*, αFLN (A1219T) staining of formaldehyde-fixed parasites; *middle*, αFLN Ab (A1219T) was preincubated with 10 μg/ml immunizing peptide; *right*, αFLN (1624T) staining of formaldehyde-fixed parasites. *C*, immunofluorescence with antibodies directed against FLN (*red*, A1219T) and BiP (*green*) after formaldehyde fixation. *Merged image* is shown on the *right*. *D*, immunofluorescence with antibodies directed against FLN (*red*, A1219T) and LWL-1 (*green*) after formaldehyde fixation. *Merged image* is shown on the *right*.

DISCUSSION

Prior to our current studies, all of the available data (8, 11) pointed to falcilysin as a food vacuole enzyme involved exclusively in hemoglobin degradation. However, the dual specificity of FLN partners well with the dual localization data. Two independent and specific αFLN antisera, under a variety of fixation conditions, document falcilysin localization to membranous structures within the parasite, in addition to the food vacuole. We cannot be sure of the identity of these membranes; there are morphologic similarities to endoplasmic reticulum, yet we observed minimal overlap in the distribution of the ER marker, BiP, and FLN. FLN staining was confined to the parasite body, because it is internal to the signal of LWL-1, a resident protein of the parasitophorous vacuolar membrane that delimits the parasite. It is possible that FLN, which lacks a signal peptide (11) and exhibits no change in localization after Brefeldin A treatment, is located in or traffics through the

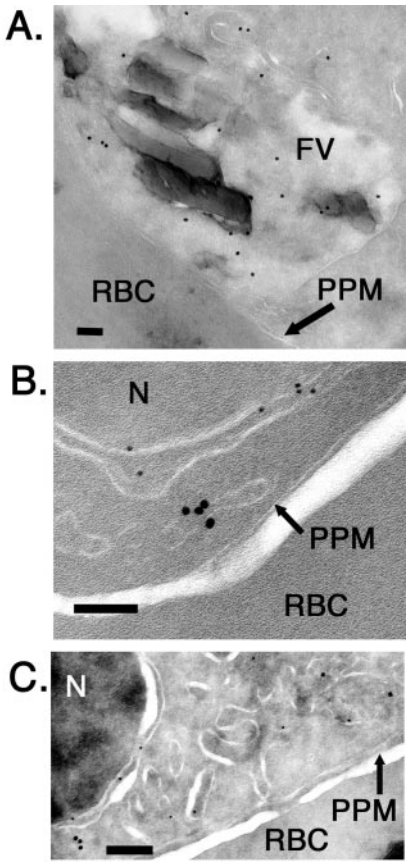

FIG. 4. **Cryo-immunoelectron microscopy with FLN.** Immunoelectron microscopy of trophozoites using αFLN. *A*, FLN staining within the food vacuole. *B* and *C*, FLN staining (18-nm gold) present in membrane-bound structures largely distinct from the distribution of the classic ER marker BiP (12-nm gold). Each *scale bar* represents 100 nm. *FV*, food vacuole; *RBC*, red blood cell; *PPM*, parasite plasma membrane; *N*, nucleus.

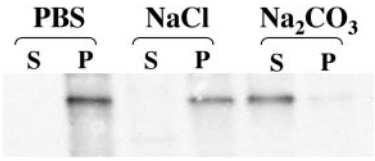

FIG. 5. **FLN is a peripheral membrane protein.** Early to mid-stage trophozoites were labeled with [^{35}S]methionine-cysteine for 4 h. Parasites were harvested, disrupted by sonication, and subjected to independent extractions in the solutions shown. After extraction, immunoprecipitations were performed with αFLN (A1219T). *S*, supernatant; *P*, pellet.

vesicles associated with the alternative secretory pathway characterized by Brefeldin A-independent secretion (26–28). Previous work analyzing the biosynthesis of falcilysin indicates that the enzyme does not require proteolytic processing to be active (11). Therefore, these data and the specificity studies suggest that FLN may be active along its targeting route or may have a resident function in these vesicles.

The random peptide libraries document that FLN is indeed active at both pH 5.2 and 7.2. This is not unprecedented for proteases. The striking finding is the pH-dependent substrate selectivity of FLN. The consensus specificity at acidic pH ((Y/A)N(E/H)(N/H)S#(Y/F/L)(M/F)M(E/D)(E/D)) has stretches of neutral polar, bulky hydrophobic, and acidic residues. At neutral pH (MK(R/G)(H/M)(S/R)#(Y/F/L)RMR*X*) positively charged residues dominate. The pH-dependent switch in substrate specificity presumably is related to protonation changes within the active site, although distal changes leading to conformational differences are also possible. A crystal structure of FLN will likely be necessary to determine the substrate-switch mechanism. The mitochondrial processing peptidase (MPP) is the only M16 metalloprotease with structural information available (29), and it provides few clues for falcilysin. MPP and FLN share a low degree of homology (8), and belong to different M16 subfamilies. Furthermore, MPP differs in that is a α/β heterodimer with the active site lying at the subunit interface (29).

Kinetic analyses of the optimized substrates validated the peptide library predictions, because catalytic efficiencies were dramatically improved compared with the standard substrate α74–75. The α74–75 peptide was originally chosen for assay development, because it was a site in globin recognized by food vacuole lysate and not characteristic for the specificity of other known globin-degrading enzymes. This peptide is cleaved successfully by FLN, but the optimized substrates determined by the peptide library analysis are three orders of magnitude better. Pacid/P′acid was recognized optimally by FLN at pH 5, but also had a smaller activity peak at pH 7. In contrast, Pneut/P′neut was a poor substrate at pH 5; it was optimal from pH 7 to 8. Thus, using some substrates one would conclude that this is an acid protease and with other substrates one would think FLN is a neutral protease. Some change in substrate preference with pH has been seen with other proteases (30), but a bold switch like that of falcilysin has not been reported. FLN is virtually one protease at acidic pH and another at neutral/basic pH.

Whether pH-dependent specificity is a general feature of metalloproteases remains to be seen. However, falcilysin has specificity similarities to other metalloproteases. Mitochondrial processing peptidase is the falcilysin family member most extensively characterized. MPP favors aromatic residues in the P1′ position (31), as does FLN. Additionally, MPP substrates often carry an Arg in the P2 or P3 position (32, 33). The FLN motif for pH 7.2 contains an Arg at P3 and His at P2. Nonrelated metalloproteases such as MMP-7 have a strong preference for Ser in the P1 position (25). Ser is the clearly favored residue in P1 for falcilysin in both acidic and neutral pH. In the metalloproteases examined by Turk *et al.* (25), also via random peptide libraries, there is very little preference similarity elsewhere in the unprimed positions, but the primed positions do exhibit modest agreement with the FLN cleavage motifs. Leu is found in P1′ in every one of the six metalloproteases they analyzed (MMP-7, MMP1, MMP-2, MMP-9, MMP-3, and MMP-14). Additionally, Arg is present in each of the proteases at the P2′ position, which concurs with the motif for FLN at pH 7.2. Finally, Met is found for three of the six metalloproteases in the P3′ position. Both FLN motifs carry a Met in this same position. Comparing the FLN cleavage residue abundance values to those determined by Turk *et al.* (25) reveals that, with the exception of P1, FLN exhibits a stronger, more robust preference for residues in all positions. Turk and colleagues used a similar library approach to determine their cleavage motifs and yet the majority of the preferred residues have abundance values less than 2.0. The bulk of the preferred residues of falcilysin have abundance values above 3 and ranging as high as 6 to 11, even at distal residues P5 and P5′. In other words, falcilysin appears to be a more specific enzyme.

In summary, we present biochemical evidence that falcilysin is active at neutral pH and is found in non-food vacuole locations. This raises the possibility of an expanded role for FLN beyond globin catabolism. This notion is further supported by data that identify FLN as part of the *Plasmodium* sporozoite transcriptome (34) and proteome (35). Hemoglobin degradation does not occur in sporozoites, and falcilysin likely plays a more

fundamental role in parasite biology. We are currently using our neutral pH specificity data to aid in the identification of non-globin FLN substrates. Biochemical and mutational analyses are also underway to dissect the mechanism of the specificity switch in this unusual protease.

Acknowledgments—We thank Dave McCourt of Midwest Analytical for the N-terminal sequencing, Kasturi Haldar for LWL-1 antibody, Wandy Beatty for preparation of the cryo-EM, and Eva Istvan for critical review of the manuscript.

REFERENCES

1. Trigg, P. A., and Kondrachine, A. V. (1998) *Malaria: Parasite Biology, Pathogenesis, and Protection* (Sherman, I. W., ed) American Society of Microbiology, Washington, D. C.
2. Banerjee, R., and Goldberg, D. E. (2001) in *Antimalarial Chemotherapy* (Rosenthal, P. J., ed) pp. 43–63, Humana Press, Totowa, NJ
3. Goldberg, D. E., Slater, A. F., Beavis, R., Chait, B., Cerami, A., and Henderson, G. B. (1991) *J. Exp. Med.* **173,** 961–969
4. Gluzman, I. Y., Francis, S. E., Oksman, A., Smith, C. E., Duffin, K. L., and Goldberg, D. E. (1994) *J. Clin. Invest.* **93,** 1602–1608
5. Gamboa de Dominguez, N. D., and Rosenthal, P. J. (1996) *Blood* **87,** 4448–4454
6. Francis, S. E., Gluzman, I., Oksman, A., Banerjee, D., and Goldberg, D. E. (1996) *Mol. Biochem. Parasitol.* **83,** 189–200
7. Sijwali, P., Shenai, B., Gut, J., Singh, A., and Rosenthal, P. (2001) *Biochem. J.* **360,** 481–489
8. Eggleson, K. K., Duffin, K. L., and Goldberg, D. E. (1999) *J. Biol. Chem.* **274,** 32411–32417
9. Krogstad, D. J., Schlesinger, P. H., and Gluzman, I. Y. (1985) *J. Cell Biol.* **101,** 2302–2309
10. Yayon, A., Cabantchik, Z. I., and Ginsburg, H. (1984) *EMBO J.* **3,** 2695–2700
11. Murata, C. E., and Goldberg, D. E. (2003) *Mol. Biochem. Parasitol.* **129,** 123–126
12. Rawlings, N. D. (1998) in *Handbook of Proteolytic Enzymes* (Barrett, A. J., Rawlings, N. D., and Woessner, J. F., eds) pp. 1360–1362, Academic Press, San Diego
13. Bohni, P., Gasser, S., Leaver, C., and Schatz, G. (1980) in *The Organization and Expression of the Mitochondrial Genome* (Kroon, A. M., and Saccone, C., eds) pp. 423–433, Elsevier Science Publishers, Amsterdam
14. Richter, S., and Lamppa, G. K. (1998) *Proc. Natl. Acad. Sci. U. S. A.* **95,** 7463–7468
15. Schmidt, G. W., Devillers-Thiery, A., Desruisseaux, H., Blobel, G., and Chua, N. H. (1979) *J. Cell Biol.* **83,** 615–622
16. Adames, N., Blundell, K., Ashby, M. N., and Boone, C. (1995) *Science* **270,** 464–467
17. Fujita, A., Oka, C., Arikawa, Y., Katagai, T., Tonouchi, A., Kuhara, S., and Misumi, Y. (1994) *Nature* **372,** 567–570
18. Shii, K., Yokono, K., Baba, S., and Roth, R. A. (1986) *Diabetes* **35,** 675–683
19. Gehm, B. D., and Rosner, M. R. (1991) *Endocrinology* **128,** 1603–1610
20. Trager, W., and Jensen, J. B. (1976) *Science* **193,** 673–675
21. Lambros, C., and Vanderberg, J. P. (1979) *J. Parasitol.* **65,** 418–420
22. Banerjee, R., Liu, J., Beatty, W., Pelosof, L., Klemba, M., and Goldberg, D. E. (2002) *Proc. Natl. Acad. Sci. U. S. A.* **99,** 990–995
23. Francis, S. E., Banerjee, R., and Goldberg, D. E. (1997) *J. Biol. Chem.* **272,** 14961–14968
24. Matayoshi, E. D., Wang, G. T., Krafft, G. A., and Erickson, J. W. (1990) *Science* **247,** 954–958
25. Turk, B. E., Huang, L. L., Piro, E. T., and Cantley, L. C. (2001) *Nat. Biotechnol.* **19,** 661–667
26. Lingelbach, K. (1993) *Exp. Parasitol.* **76,** 318–327
27. Foley, M., and Tilley, L. (1998) *Int. J. Parasitol.* **28,** 1671–1680
28. Shahabuddin, M., Gunther, K., Lingelbach, K., Aikawa, M., Schreiber, M., Ridley, R. G., and Scaife, J. G. (1992) *Exp. Parasitol.* **74,** 11–19
29. Taylor, A. B., Smith, B. S., Kitada, S., Kojima, K., Miyaura, H., Otwinowski, Z., Ito, A., and Deisenhofer, J. (2001) *Structure* (*Camb*) **9,** 615–625
30. Gillmor, S. A., Craik, C. S., and Fletterick, R. J. (1997) *Protein Sci.* **6,** 1603–1611
31. Ogishima, T., Niidome, T., Shimokata, K., Kitada, S., and Ito, A. (1995) *J. Biol. Chem.* **270,** 30322–30326
32. Kojima, K., Kitada, S., Ogishima, T., and Ito, A. (2001) *J. Biol. Chem.* **276,** 2115–2121
33. Song, M. C., Shimokata, K., Kitada, S., Ogishima, T., and Ito, A. (1996) *J. Biochem.* (*Tokyo*) **120,** 1163–1166
34. Kappe, S. H., Gardner, M. J., Brown, S. M., Ross, J., Matuschewski, K., Ribeiro, J. M., Adams, J. H., Quackenbush, J., Cho, J. K., Carruci, D. J., Hoffman, S. L., and Nussenzweig, V. (2001) *Proc. Natl. Acad. Sci. U. S. A.* **98,** 9895–9900
35. Florens, L., Washburn, M. P., Raine, J. D., Anthony, R. M., Grainger, M., Haynes, J. D., Moch, J. K., Muster, N., Sacci, J. B., Tabb, D. L., Witney, A. A., Wolters, D., Wu, Y., Gardner, M. J., Holder, A. A., Sinden, R. E., Yates, J. R., and Carucci, D. J. (2002) *Nature* **419,** 520–526